APPLIED AND ENVIRONMENTAL MICROBIOLOGY, Feb. 2010, p. 866–879 Vol. 76, No. 3
0099-2240/10/$12.00 doi:10.1128/AEM.02009-09

Diversity and Evolution of the Phenazine Biosynthesis Pathway▽†

Dmitri V. Mavrodi,[1]* Tobin L. Peever,[1] Olga V. Mavrodi,[1] James A. Parejko,[2] Jos M. Raaijmakers,[3] Philippe Lemanceau,[4] Sylvie Mazurier,[4] Lutz Heide,[5] Wulf Blankenfeldt,[6] David M. Weller,[7] and Linda S. Thomashow[7]

Department of Plant Pathology, Washington State University, Pullman, Washington 99164-6430[1]; School of Molecular Biosciences, Washington State University, Pullman, Washington 99164-4234[2]; Laboratory of Phytopathology, Wageningen University, Binnenhaven 5, P.O. Box 8025, 6709 PD Wageningen, the Netherlands[3]; UMR Microbiologie et Géochimie des Sols, INRA/Université de Bourgogne, CMSE, BP 86510, 17 Rue Sully, 21065 Dijon Cedex, France[4]; Pharmaceutical Institute, Eberhard-Karls-Universität Tübingen, Auf der Morgenstelle 8, 72076 Tübingen, Germany[5]; Max Planck Institute of Molecular Physiology, Otto-Hahn-Str. 11, 44227 Dortmund, Germany[6]; and USDA-ARS, Root Disease and Biological Control Research Unit, Washington State University, Pullman, Washington 99164-6430[7]

Received 20 August 2009/Accepted 1 December 2009

Phenazines are versatile secondary metabolites of bacterial origin that function in biological control of plant pathogens and contribute to the ecological fitness and pathogenicity of the producing strains. In this study, we employed a collection of 94 strains having various geographic, environmental, and clinical origins to study the distribution and evolution of phenazine genes in members of the genera *Pseudomonas*, *Burkholderia*, *Pectobacterium*, *Brevibacterium*, and *Streptomyces*. Our results confirmed the diversity of phenazine producers and revealed that most of them appear to be soil-dwelling and/or plant-associated species. Genome analyses and comparisons of phylogenies inferred from sequences of the key phenazine biosynthesis (*phzF*) and housekeeping (*rrs*, *recA*, *rpoB*, *atpD*, and *gyrB*) genes revealed that the evolution and dispersal of phenazine genes are driven by mechanisms ranging from conservation in *Pseudomonas* spp. to horizontal gene transfer in *Burkholderia* spp. and *Pectobacterium* spp. DNA extracted from cereal crop rhizospheres and screened for the presence of *phzF* contained sequences consistent with the presence of a diverse population of phenazine producers in commercial farm fields located in central Washington state, which provided the first evidence of United States soils enriched in indigenous phenazine-producing bacteria.

The naturally occurring phenazines include more than 50 nitrogen-containing heterocyclic pigments of bacterial origin (36). They have characteristic absorption spectra with two peaks in the UV range and at least one peak in the visible range that determines their colors (42). Almost all phenazines are broadly inhibitory to the growth of bacteria and fungi due to their ability to undergo cellular redox cycling in the presence of oxygen and reducing agents (including NADH and NADPH) and cause the accumulation of toxic superoxide and hydrogen peroxide (42). Phenazine-1-carboxylic acid (PCA), 2-hydroxyphenazine-1-carboxylic acid, and phenazine-1-carboxamide (PCN) produced in the rhizosphere by *Pseudomonas fluorescens* and *Pseudomonas chlororaphis* inhibit soilborne phytopathogenic fungi (13, 62) and contribute to the natural suppression of *Fusarium* wilt disease in certain soils in France (45). Phenazines produced by *Pantoea agglomerans* on apple flowers contribute to suppression of phytopathogenic *Erwinia amylovora*, which causes fire blight disease (22). Production of pyocyanin (PYO) by *Pseudomonas aeruginosa* is required for generation of disease symptoms in plants and killing of the nematode *Caenorhabditis elegans* and the fruit fly *Drosophila melanogaster* (40, 54), and it is also critical for lung infection by *P. aeruginosa* in mice (35). In contrast, some phenazines produced by *Streptomyces* spp. are not cytotoxic in eukaryotes and have promise as anticancer or anti-infective drugs (36).

In addition to the effects of phenazines on other organisms, recent studies have indicated that these compounds directly activate certain transcription factors and act as intercellular signals in *P. aeruginosa* (17, 18, 53). Because of their redox properties, phenazines also can function in the physiology of the strains that produce them by mediating the reoxidation of NADH under oxygen-limiting conditions, such as those found in mature biofilms (39, 53). In soil, phenazines can promote microbial mineral reduction and may function as electron shuttles, facilitating bacterial and plant access to iron and nutrients such as phosphate, trace minerals, and organic compounds associated with mineral phases (26). Several studies have demonstrated that phenazines are beneficial for the competitiveness and long-term survival of the producers in natural habitats. Strains of *Pseudomonas* that synthesized phenazines were more competitive and survived longer on the roots of wheat than non-phenazine-producing mutants (46). Similarly, PYO-deficient mutants were less competitive and less virulent than wild-type *P. aeruginosa* in mouse acute and chronic pneumonia infection models (35).

Over the past decade, significant progress has been made toward understanding the enzymatic steps leading to the assembly of the phenazine scaffold, but our knowledge of the diversity of phenazine-producing bacteria and the evolution of

* Corresponding author. Mailing address: Department of Plant Pathology, Washington State University, Pullman, WA 99164-6430. Phone: (509) 335-3269. Fax: (509) 335-7674. E-mail: mavrodi@mail.wsu.edu.

† Supplemental material for this article may be found at http://aem.asm.org/.

▽ Published ahead of print on 11 December 2009.

phenazine (Phz) biosynthesis pathways is limited. Except for the archaebacterium *Methanosarcina mazei*, which utilizes an unusual membrane-bound phenazine as an electron carrier in methanogenesis (1), phenazine biosynthesis is limited to bacteria (36, 64), and the ability to produce phenazines occurs in the *Actinobacteria* and two clades (*Betaproteobacteria* and *Gammaproteobacteria*) of Gram-negative *Proteobacteria* (42, 64). Previously, the evolution of the phenazine pathway was investigated in a single study that focused only on sequenced microbial genomes (19). This study found that phenazine genes have a complex evolutionary history and that horizontal gene transfer likely occurs. In the present study, we utilized improved phenazine gene-specific probes and a large collection of strains having diverse geographic, environmental, and clinical origins to assess the distribution of phenazine genes in economically important groups of bacteria and to gain insight into habitats that support phenazine producers. We also studied the evolution of the phenazine pathway in different groups of bacteria by carrying out genome analyses and comparing phylogenies inferred from sequences of the key phenazine biosynthesis (*phzF*) and housekeeping genes. Finally, we collected samples of cereal crops grown in central Washington state and screened them for the presence of phenazine producers. Our results (i) confirmed the extensive diversity of phenazine-producing bacteria; (ii) suggested that most phenazine producers are soil-dwelling and/or plant-associated species; (iii) revealed that different molecular mechanisms are involved in the evolution and dispersal of phenazine pathways in different lineages of bacteria; and (iv) revealed diversity among phenazine producers in commercial farm fields located in central Washington, which provided evidence of a United States soil enriched in indigenous phenazine-producing bacteria.

MATERIALS AND METHODS

Bacterial strains and growth conditions. Bacterial strains used in this study are described in Table 1. These bacteria included strains belonging to the genera *Pseudomonas* ($n = 51$), *Burkholderia* ($n = 27$), *Brevibacterium* ($n = 3$), *Streptomyces* ($n = 1$), and *Pectobacterium* ($n = 12$) and having environmental and clinical origins, as well as strains received from the American Type Culture Collection (ATCC) (Manassas, VA). All strains were grown at 28°C. *Pseudomonas* spp., *Burkholderia* spp., and *Pectobacterium* spp. were grown in Luria-Bertani (LB) broth (5). *Brevibacterium* spp. and *Streptomyces cinnamonensis* were cultured in nutrient broth (BD Biosciences, Franklin Lakes, NJ) and yeast extract-malt extract broth (BD Biosciences), respectively.

Amplification and sequencing of target genes. Total DNA was extracted from bacteria by using a cetyltrimethylammonium bromide (CTAB) miniprep procedure (5). For *Brevibacterium* spp. and *S. cinnamonensis*, the protocol was modified by pretreating the biomass for 30 min at room temperature with lysozyme (final concentration, 1 mg · ml^{-1}) prior to addition of SDS. DNA concentrations were measured by using a DNA quantitation kit (Bio-Rad, Hercules, CA).

Oligonucleotide primers targeting conserved regions in genes of interest were designed with the Oligo v. 6.71 software (Molecular Biology Insights, Inc., West Cascade, CO). Amplification was performed with a PTC-200 gradient thermal cycler (Bio-Rad) using GoTaq DNA polymerase (Promega, Inc., Madison, WI). The annealing temperature (Table 2) was optimized for each primer pair and, if necessary, 5% dimethyl sulfoxide was added to PCR mixtures. Amplification products were cleaned with QIAquick PCR purification spin columns (Qiagen, Valencia, CA) and sequenced with a BigDye Terminator v. 3.1 cycle sequencing kit (Applied Biosystems, Foster City, CA) used according to the manufacturer's recommendations.

The following combinations of oligonucleotide primers were used to target *phzF* in different groups of bacteria: primers Ps_up1 and Ps_low1 for *Pseudomonas* spp., primers Bcep_up and Ps_low2 for *Burkholderia* spp., primers Ecar_up and Ecar_low and primers Paggl_up and Paggl_low for *Pectobacterium* spp., primers Br_up and Br_low for *Brevibacterium* spp., and primers Ps_up1 and Ps_low2 for *Streptomyces* spp. (Table 2).

Housekeeping genes for phylogenetic inference were amplified as follows. A single lower primer, recArps, was used in combination with upper primers recAf1, recAfcep, and recAfcoli to amplify *recA* in *Pseudomonas*, *Burkholderia*, and *Pectobacterium*, respectively. The homologous gene in *Brevibacterium iodinum* and *S. cinnamonensis* was targeted with primers recAfbr and recArbr (Table 2). Primers rpoBup and rpoBlow were used to amplify the 740- to 749-bp fragment of *rpoB* in *P. aeruginosa*, *P. chlororaphis*, *Burkholderia* spp., *Pectobacterium carotovorum*, *B. iodinum*, and *S. cinnamonensis*, while in the rest of the strains this gene was amplified with primers rpoBup1 and rpoBlow1. To amplify *atpD*, the lower primer atpDlow was used in combination with the upper primer atpDup1 for all species except *Pectobacterium* species, for which amplification was performed with the upper primer atpDup2 (Table 2). Finally, *gyrB* was amplified from the Gram-negative species included in this study (i.e., *Pseudomonas* spp., *Burkholderia* spp., and *Pectobacterium* spp.) with primers Up-1G− and Up-2G−, while PCRs with Gram-positive *Brevibacterium* and *Streptomyces* species were performed with primers Up-1G+ and Up-2G+ (Table 2).

Due to the length of the *rrs* amplicons, four internal primers were used for sequencing in addition to the upper and lower primers 8F and 1492R (66). The *rrs* amplicons from *Pseudomonas* spp. were sequenced with internal primers 16Sps1, r16Sps1, 16Sps2, and r16Sps2. The *rrs* PCR products from *Burkholderia* spp., *Brevibacterium* spp., *P. carotovorum*, and *S. cinnamonensis* were sequenced with internal primers 16Sps3, r16Sps3, 16Sps4, and r16Sps4 (Table 2). Sequence data were assembled and analyzed by using Vector NTI Advance v. 10 (Invitrogen Corp., Carlsbad, CA) and Omiga v. 2.0 (Accelrys, Inc., San Diego, CA).

Purification and analysis of rhizosphere DNA and isolation of root-associated Phz$^+$ bacteria. Plants with adhering soil were collected in triplicate from global positioning system (GPS)-tagged sites (Table 3), placed in plastic bags, transported to the laboratory, and stored at 4°C for no more than 24 h before processing as described below. DNA was extracted from plant root washes with a PowerSoil DNA isolation kit (MO BIO Laboratories, Carlsbad, CA) using the alternative protocol for wet soil. Briefly, the root system with adhering rhizosphere soil was placed in 10 ml of sterile distilled water, vortexed, and sonicated, and then 2 ml of the soil suspension was used for DNA extraction as described in the manufacturer's protocol. Rhizosphere DNA was quantified and screened for the presence of indigenous phenazine-producing bacteria by performing PCR with *phzF*-specific primers essentially as described above. For cloning and sequencing, PCR products were separated by gel electrophoresis, extracted from agarose by using a QIAEX II kit (Qiagen, Valencia, CA), and cloned using a pGEM-T Easy cloning system (Promega), and randomly chosen recombinant clones were sequenced with the M13 forward primer.

Selected plant root washes were also used for isolation of indigenous phenazine-producing bacteria. Briefly, 100 μl of a root wash was serially diluted and plated on 0.1× tryptic soy (BD Biosciences) and 0.33× King's B (31) media amended with cycloheximide (100 μg ml^{-1}). Plates were incubated at room temperature, and after 48 h representative morphotypes were replated and screened by performing PCR with *phzF*-specific primers. Positive isolates were stored at −80°C as glycerol stocks.

DNA hybridization-based screening of *Burkholderia* spp. Genomic DNA samples from *Burkholderia* spp. were transferred onto BrightStar-Plus positively charged nylon (Ambion, Austin, TX) with a dot blot vacuum manifold, and the bound DNA was denatured, neutralized, and immobilized by baking essentially as described by Ausubel et al. (5). Three *Burkholderia*-specific *phz* hybridization probes were prepared from *Burkholderia lata* 383 by performing PCR with primer pairs cep11/phzAcelow, cep14/phzFcep_low, and cep17/cep10 (Table 2). Prior to labeling, PCR products were cleaned by using QIAquick PCR purification spin columns (Qiagen). Probe labeling, prehybridization and hybridization at 42°C, and subsequent detection of DNA-DNA hybrids were carried out with a DIG-High Prime II DNA labeling and detection starter kit (Roche Applied Science, Indianapolis, IN) used according to the manufacturer's recommendations.

Thin-layer chromatography detection of phenazine production. Bacterial cultures were grown with shaking in LB or King's B broth for 48 h at 27°C, and phenazines were extracted with ethyl acetate as described previously (44). PCA extracted from *P. fluorescens* 2-79 was used as a standard. The extracts were dried, suspended in methanol, and spotted on silica gel plates (GHLF Uniplate; Analtech, Newark, DE). Chromatography was carried out as described by Thomashow et al. (63) using benzene-acetic acid (95:5), and chromatograms were examined at 254 nm.

Phylogenetic inference. The deduced protein sequences were aligned using Clustal X v.2.0.9 (33), and the resultant alignments were further edited with reference to protein folds predicted by the fold recognition program Phyre (8).

TABLE 1. Origins and relevant phenotypes of bacterial strains used in this study

Strain(s)[a]	Origin and relevant phenotype[b]	*phzF*[c]	Reference(s) or source
Brevibacterium iodinum			
ATCC 15728	Phz$^+$; produces iodinin	+	64
ATCC 15729	Phz$^+$; produces iodinin	+	American Type Culture Collection
ATCC 9897	Milk isolate, UK; Phz$^+$; produces iodinin	+	American Type Culture Collection
Burkholderia sp.			
PC-4	Lettuce rhizosphere isolate, Japan	+	56
PC-5	Lettuce rhizosphere isolate, Japan	−	56
PC-8	Chinese cabbage rhizosphere isolate, Japan	+	56
PC-14, PC-17, PC-19	Welsh onion rhizosphere isolates, Japan	+	56
PC-22	Soybean rhizosphere isolate, Japan	+	56
PC-28, PC-30, PC-33	Barley rhizosphere isolates, Japan	+	56
PC-29	Barley rhizosphere isolate, Japan	−	56
PC-39, PC-42, PC-43	Tobacco rhizosphere isolates, Japan	+	56
683	Clinical isolate, Japan	−	56
2424	Japan	+	56
ATCC 1746, H1 2468	Clinical isolates, USA	−	Gee W. Lau
5.5B	Soil isolate, USA; Phz$^+$; produces 4,9-dihydroxy phenazine-1,6-dicarboxylic acid dimethyl ester	+	11
***Burkholderia lata* 383**	Soil isolate, Trinidad; Phz$^+$	+	58
Burkholderia cepacia ATCC 25416	Onion isolate, USA	−	41
Burkholderia cenocepacia K56-2	Genomovar III clinical isolate, Canada	−	41
Burkholderia stabilis LMG14294	Genomovar IV clinical isolate, Belgium	−	41
Burkholderia dolosa LMG18943	Genomovar VI clinical isolate, USA	−	16
Burkholderia ambifaria LMG21821	Genomovar VIII clinical isolate, USA	−	16
Burkholderia vietnamiensis PC259	Clinical isolate, Washington state	−	34
Burkholderia phenazinium ATCC 33666	Soil isolate; Phz$^+$; produces iodinin	−	64
***Pectobacterium atrosepticum* SCRI1043**	Potato isolate, Scotland	+	7
Pectobacterium betavasculorum Ecb168	Sugar beet isolate, USA	+	6
Pectobacterium carotovorum			
cc101, cc102, cc104, cc106, cc108, cc110, cc505	Potato seed isolates, USA	−	10
cc303	Soil isolate, Oregon	+	10
cc306	Soil isolate, Oregon	−	10
cc501	Potato stem isolate	−	10
Pseudomonas aeruginosa			
PAO1	Clinical isolate, Australia; Phz$^+$; produces PYO	+	Pseudomonas Genetic Stock Center
ATCC 23993	Clinical isolate, Japan; Phz$^+$; produces PYO	+	American Type Culture Collection
ATCC 25007	Phz$^+$; produces PYO	+	American Type Culture Collection
ATCC 25011	Clinical isolate, Japan; Phz$^+$; produces aeruginosins A and B	+	American Type Culture Collection
PAK	Phz$^+$; produces PYO	+	Lab collection
SC-1, SC-8	Environmental isolates, India; Phz$^+$; produce PYO	+	Shaji Philip
CF10, CF17, CF40, CF51, CF54, CF57, CF62, CF76, CF89	Clinical isolates, USA; Phz$^+$; produce PYO	+	Gee W. Lau
Pseudomonas chlororaphis subsp. *aureofaciens*			
30-84	Soil isolate, USA; Phz$^+$; produces PCA, 2-OH-PCA, and 2-OH-PHZ	+	Lab collection
ATCC 17415	Soil isolate, USA; Phz$^+$; produces PCA, 2-OH-PCA, and 2-OH-PHZ	+	58
ATCC 13985	Maas River clay isolate, the Netherlands; Phz$^+$; produces PCA, 2-OH-PCA, and 2-OH-PHZ	+	58
TX-1	Turfgrass soil isolate, Michigan; Phz$^+$; produces PCA, 2-OH-PCA, and 2-OH-PHZ	+	Eco Soils Systems, Inc., San Diego, CA
BS1391, **BS1393**	Soil isolates, Russia; Phz$^+$; produce PCA, 2-OH-PCA, and 2-OH-PHZ	+	Lab collection
PGS12	Corn rhizosphere isolate, USA; Phz$^+$; produces PCA, 2-OH-PCA, and 2-OH-PHZ	+	20

Continued on following page

TABLE 1—*Continued*

Strain(s)[a]	Origin and relevant phenotype[b]	*phzF*[c]	Reference(s) or source
Pseudomonas chlororaphis subsp. *chlororaphis*			
ATCC 17411	Phz$^+$; produces PCN	+	58, 64
ATCC 17809	Phz$^+$; produces PCN	+	58
ATCC 9446	Plate contaminant; Phz$^+$; produces PCN	+	58
***Pseudomonas fluorescens* 2-79**	Wheat rhizosphere isolate, Washington state; Phz$^+$; produces PCA	+	67
Pseudomonas sp.			
C1Phz19, C1Phz22, **C1Phz26**, C1Phz47, CHLR105, CHTR224, SLPH10	*Fusarium* wilt-suppressive soil isolates, Châteaurenard, France	+	Philippe Lemanceau
	Take-all decline soil isolate, the Netherlands	+	Jos Raaijmakers
CMR5c, CMR12a	Cocoyam rhizosphere isolates, Cameroon; Phz$^+$; produce PCN	+	49
R2-6-07, **R2-7-07,** R2-10-07, R2-12-07, R2-13-07, R2-30-07, **R4-**34**-07, R4-35-07,** R5-89-07, **R5-90-07, R11-23-07, R11-45-07, R14-24-07,** R15-2-07, **L1-11-07**	Wheat rhizosphere isolates, Washington state; Phz$^+$; produce PCA	+	This study
***Streptomyces cinnamonensis* DSM1042**	Soil isolate; Phz$^+$; produces PCA and endophenazines A and B	+	24

[a] Bold type indicates phenazine producers that form a subset of 31 strains that was used for contrasting the phylogenies of *phzF* and housekeeping genes.
[b] Phz$^+$, strain produces phenazines; iodinin, 1,6-dihydroxyphenazine-5,10-di-*N*-oxide; PYO, pyocyanin (5-methyl-1-hydroxyphenazinium betaine); PCA, phenazine-1-carboxylic acid; PCN, phenazine-1-carboxamide; 2-OH-PCA, 2-hydroxyphenazine-1-carboxylic acid; 2-OH-PHZ, 2-hydroxyphenazine; aeruginosin A, 5-methyl-7-amino-1-carboxyphenazinium betaine; aeruginosin B, 5-methyl-7-amino-1-carboxy-3-sulfophenazinium; endophenazine A, 9-(3-methyl-2-butenyl)phenazine-1-carboxylic acid; endophenazine B, 1-carboxy-5-methyl-9-(3-methyl-2-butenyl)-phenazin-7-one; UK, United Kingdom; USA, United States.
[c] Results of PCR-based detection of *phzF* with primers listed in Table 2.

The refined amino acid alignments were then used to align the corresponding nucleotide sequences using CodonAlign v.2 (25).

Molecular Evolutionary Genetics Analysis software (MEGA) version 4.0.2 (61) was used to infer trees based on neighbor joining of genetic distances (NJ) and maximum parsimony (MP). The NJ method was used with DNA and protein distances corrected by using the Kimura two-parameter (30) and Jones-Taylor-Thornton (29) models of evolution, respectively. For MP analyses, the close-neighbor interchange algorithm was used, and an initial tree was generated by random addition of the sequences. The reproducibility of clades in the inferred NJ and MP trees was assessed by bootstrap resampling with 1,000 replicates.

For maximum likelihood (ML) and Bayesian analyses, sequences for each locus were aligned and collapsed into haplotypes by removing indels and infinite-site violations with the Map program and phylogenetically incompatible sites with the Clade, Matrix, and CladeEx programs implemented in SNAP Workbench (52). Models of sequence evolution were evaluated for each data set and the combined data set using Modeltest v.3.7 implemented in PAUP v. 4.10b10 (60) and the Modeltest server (51). The Akaike information criterion (3) was used to select the most appropriate evolutionary model for each data set. ML phylogenies were estimated independently for each data set (*phzF*, *rrs*, *atpD*, *gyrB*, *recA*, and *rpoB*) and for the combined housekeeping gene data set (*rrs*, *atpD*, *gyrB*, *recA*, and *rpoB*) by using heuristic searches in PAUP. The reproducibility of clades was assessed by using heuristic searches of 1,000 bootstrapped data sets with "fast" stepwise addition of taxa and no branch swapping. To assess the suitability of combining the *rrs*, *atpD*, *gyrB*, *recA*, and *rpoB* data sets for phylogenetic analysis, a "conditional data combination" approach (27) was employed. Incongruence among partitions was assessed with a Shimodaira-Hasegawa (SH) test (57) implemented in PAUP using 1,000 bootstrapped replicates with RELL approximation of likelihood. The tests compared the topologies of the ML consensus trees estimated for each partition to the topology of the combined (concatenated) ML consensus tree.

ML phylogenies were also estimated for the combined and *phzF* data sets in a Bayesian framework using MrBayes version 3.1 (28). Flat Dirichlet probability densities were used as priors for the substitution rate parameters, and stationary nucleotide frequencies and uniform priors were used for the shape and topology parameters. An exponential unconstrained prior was used for the branch length parameter. Each analysis consisted of two runs of the Markov chain started from a random tree with 1,000,000 generations per run, six chains employed in each run, and random chains swapped three times per generation. Trees were sampled every 100 generations, and the first 50,000 generations of each analysis were discarded as burn-in. Average posterior probabilities were estimated for each node of the phylogeny across the two runs (19,000 trees from 2,000,000 total generations of the Markov Chain Monte Carlo).

Genome analyses. Genome-scale analyses of phenazine biosynthesis locus organization were performed using the *Pseudomonas* (http://v2.pseudomonas.com/index.jsp) and *Burkholderia* (http://burkholderia.com/index.jsp) online genome databases, as well as the microbial genome resources section of GenBank (http://www.ncbi.nlm.nih.gov/genomes/lproks.cgi). Comparisons of genome regions flanking phenazine biosynthesis operons were performed with web-based implementation (WebACT) of the Artemis comparison tool (12).

Nucleotide sequence accession numbers. Sequence data have been deposited in the GenBank database under the following accession numbers: FJ652597 through FJ652623 for *rrs*; FJ652624 through FJ652650 for *recA*; FJ652651 through FJ652677 for *atpD*; FJ652678 through FJ652704 for *rpoB*; FJ652705 through FJ652731 for *gyrB*; and FJ652732 through FJ652786 for *phzF*. Other GenBank entries used in this study include (i) the *phzF* gene from *Streptomyces anulatus* LU9663 (accession no. FN178498); (ii) *rrs* genes from *P. chlororaphis* ATCC 13985 (accession no. AF094722) and *P. chlororaphis* ATCC 9446 (accession no. AF094723); (iii) phenazine biosynthesis operons from *P. fluorescens* 2-79 (accession no. L48616), *P. chlororaphis* PCL1391 (accession no. AF195615), *P. chlororaphis* 30-84 (accession no. L48339 and AF007801), *P. agglomerans* Eh1087 (accession no. AF451953), and *S. cinnamonensis* DSM1042 (accession no. AM384985); (iv) sequenced microbial genomes of *P. aeruginosa* PAO1 (accession no. AE004091), *P. aeruginosa* PA7 (accession no. CP000744), *P. aeruginosa* UCBPP-PA14 (accession no. CP000438), *P. aeruginosa* 2192 (accession no. AAKW00000000), *P. aeruginosa* C3719 (accession no. AAKV00000000), *P. aeruginosa* LESB58 (accession no. FM209186), *P. fluorescens* Pf-5 (accession no. CP000076), *B. lata* 383 (accession no. CP000152), *Burkholderia glumae* BGR-1 (accession no. CP001504), *Pectobacterium atrosepticum* SCRI1043 (accession no. BX950851), *Brevibacterium linens* BL2 (accession no. AAGP00000000), and *Nocardiopsis dassonvillei* subsp. *dassonvillei* DSM 43111 (accession no. ABUI00000000).

RESULTS

Design of *phzF*-specific oligonucleotide primers. A set of phenazine-specific PCR primers was developed based on a comparison of the *phzF* gene sequences from *P. fluorescens* 2-79, *P. aeruginosa* PAO1, *B. lata* 383, *P. agglomerans* Eh1087,

TABLE 2. Target genes and PCR and sequencing primers used in this study

Gene	Putative gene function	Amplicon size (bp)	Primer	Primer sequence (5′–3′)	Melting temp (°C)[a]	Annealing temp (°C)[b]
phzF	Phenazine biosynthesis enzyme	427	Ps_up1	ATCTTCACCCCGGTCAACG	67.3	57
			Ps_low1	CCRTAGGCCGGTGAGAAC	62.2–65.5	57
		427	Bcep_up	ATCTTTACGCCGGTCAACG	65.0	57
			Ps_low2	CCRTAGGCCGGCGAGAAC	67.0–70.0	57
		439	Ecar_up	ATTTTTACCCCCGTAAATG	59.6	50
			Ecar_low	CCRTAAGCAGGAGAAAAC	54.1–57.4	50
		427	Paggl_up	ATTTTCACGCCCGTCAATG	66.2	50
			Paggl_low	CCRTAAGCTGGTGAGAAC	54.0–57.5	50
		421	Br_up	ATATTCAGCCCTGTGAACG	60.2	50
			Br_low	CCATATGCCGGGGAGAAC	65.3	50
rrs	Small-subunit rRNA	1,500	8F	AGAGTTTGATCCTGGCTCAG	61.2	55
			1492R	TACGGHTACCTTGTTACGACTT	61.6–64.0	55
			16Sps1	GTAACTGGTCTGAGAGGATG	55.7	50
			r16Sps1	CATCCTCTCAGACCAGTTAC	55.7	50
			16Sps2	GACTGCCGGTGACAAAC	58.0	50
			r16Sps2	GTTTGTCACCGGCAGTC	58.0	50
			16Sps3	CACACTGGRACTGAGACACG	60.7–63.3	50
			r16Sps3	CGTGTCTCAGTYCCAGTGTG	60.7–63.3	50
			16Sps4	AGGAAGGTGGGGAYGACG	64.4–67.1	50
			r16Sps4	CATCCCCACCTTCCTCCG	67.5	50
recA	Recombinase A	598	recAf1	TGGCTGCGGCCCTGGGTCAGATC	83.1	61
			recArps	GGTGGTTTCCGGGYTRCC	66.7–72.6	
		601[c]	recAfcep	GCCGCCGCRCTYGCCCAGATC	80.0–86.4	61
		598[c]	recAfcoli	GCGGCAGCACTGGGCCAYAT	74.8–77.9	61
		598	recAfbr	TCGACGCCGCACTGGSWCAGAT	76.7–79.7	61
			recArbr	GGTGGTCTCCGGRGAGCC	67.4–71.5	
rpoB	β Subunit of RNA polymerase	740	rpoBup	GACATCGACCACYTSGGCAACC	71.2–75.5	62
			rpoBlow	ACGGCCTGACGYWKCATGTTCG	74.0–79.2	
		740	rpoBup1	GACATCGAYCACCTGGGYAACC	67.9–75.3	62
			rpoBlow1	ACRGCCTGACGCTGCATGTTSG	73.0–79.2	
atpD	β Subunit of ATP synthase	608[c]	atpDup1	GGTGTGGGYGAGCGYACYCGTG	72.1–85.2	62
		608[c]	atpDup2	GGCGTKGGYGAGCGYACCCGTG	78.5–88.7	
			atpDlow	TCSATRCCSAGGATCGCRATGATGTC	68.1–83.6	
gyrB	DNA gyrase subunit B	1,208	Up-1G-	YGCSGGCGGYAAGTTCGA	65.2–77.7	60
			UP-2G-	CCRTCGACGTCVGCRTCGGT	69.7–80.0	
		1,268	Up-1G+	CGCSGGCGGYAAGTTCGG	69.5–79.3	60
			UP-2G+	CCGTCGACRTCSGCGTCSGC	71.0–82.5	
phzA	Phenazine gene from *B. lata* 383	1,496	cep11	GGGCAACTACATGATCGG	60.8	57
			phzAcelow	TTTTTGGATCCATTGGGTATGCGTTAG	76.0	57
phzEF	Phenazine genes from *B. lata* 383	2,495	cep14	ACATGGTGCTCGACGAAG	61.1	57
			phzFceplow	TTTTGGATCCGCTAGACGCCCAG	76.7	57
phzC	Phenazine gene from *B. lata* 383	3,031	cep17	CATCATCGCCTTCAAACG	62.1	57
			cep10	TTTTGGATCCGCTACGCATACGCC	78.4	57

[a] Melting temperatures were calculated using the nearest-neighbor method implemented in Oligo v.6.71.
[b] Annealing temperatures used for PCR amplification.
[c] Two different upper primers were used in combination with a single lower primer.

P. atrosepticum SCRI1043, and *B. linens* BL2. The *phzF* gene encodes an enzyme involved in isomerization of the phenazine precursor *trans*-2,3-dihydro-3-hydroxyanthranilic acid to a highly reactive ketone (9). *phzF* is required for phenazine biosynthesis and is highly conserved in all known phenazine producers (42). PhzF is a member of a large protein superfamily that also includes diaminopimelate epimerases, proline racemases, and the 2-methylaconitate isomerase PrpF. However, because the constraints at the nucleotide level are much more relaxed than those at the amino acid level, it was possible to design primers specifically targeting enzymes involved in synthesis of phenazines. Initial efforts to develop "universal" oligonucleotide primers that would efficiently amplify *phzF* in all known phenazine-producing genera were unsuccessful due to the high degree of nucleotide variation among *phzF* alleles (data not shown). Instead, we designed genus-specific primer sets (Table 2) that have different sequences but target the same region of *phzF*. The 5′ ends of these primers complement

TABLE 3. Detection of *phzF* in DNA samples extracted from the rhizospheres of crops collected in wheat-producing areas of Washington state

Sample	Crop	Site description	Geographic coordinates	Sampling date (mo/day/yr)	*phzF*[a]
1	Alfalfa	Commercial farm field west of Ritzville, WA	47°8′27″N, 118°28′17″W	4/22/07	+
2	Winter wheat	Commercial farm field west of Ritzville, WA	47°8′32″N, 118°28′26″W	4/22/07	+
3	Spring wheat	Experimental plot with continuous soft white spring wheat west of Ritzville, WA	47°8′35″N, 118°28′18″W	5/23/08	+
4	Spring wheat	Experimental plot with continuous hard white spring wheat west of Ritzville, WA	47°8′35″N, 118°28′18 ″W	5/23/08	+
5	Spring barley	Experimental plot with spring barley-soft white spring wheat rotation west of Ritzville, WA	47°8′35″N, 118°28′18″W	5/23/08	+
6	Winter wheat	Commercial farm field west of Ritzville, WA	47°8′34″N, 118°28′22″W	6/15/09	+
7	Winter wheat	Commercial farm field west of Ritzville, WA	47°7′56″N, 118°34′26″W	6/15/09	+
8	Winter wheat	Commercial farm field west of Ritzville, WA	47°12′20″N, 118°34′41″W	6/15/09	+
9	Winter wheat	Commercial farm field west of Ritzville, WA	47°12′25″N, 118°26′59″W	6/15/09	+
10	Winter wheat	Commercial field south of Lind, WA	46°54′45″N, 118°33′58″W	4/21/09	+
11	Winter wheat	Commercial field south of Lind, WA	46°47′40″N, 118°35′21″W	4/21/09	+

[a] Results of PCR-based detection of *phzF*$^+$ rhizobacteria with primers listed in Table 2.

positions 184 and 611 in the *phzF* DNA sequence of *P. fluorescens* 2-79. At the protein level the primers encompass two short stretches of invariant amino acids that are located adjacent to the active center residues His74 and Asp208 and form parts of the active site and intermonomer cavity.

Distribution of *phzF* in the plant rhizosphere and in strains originating from diverse environmental niches and/or geographical regions. The *phzF*-specific primers were utilized to screen DNA extracted from the rhizosphere of crops sampled in late 2007 and in 2008 and 2009 at 11 GPS-tagged sites located near Ritzville and Lind, WA (Table 3). The sites selected for sampling are wheat-producing commercial farm fields typical of central Washington state and are characterized by fine, light-colored, sandy silt loam loess-derived soils with very low humic content and annual precipitation of less than 300 mm. A winter wheat-summer fallow rotation is the dominant cropping system in this region. The results of the PCR-based screening revealed the presence of phenazine sequences in all of the locations and all of the crops sampled, including winter wheat, alfalfa, spring wheat, and spring barley (Table 3).

The new *phzF*-specific primers were also used to screen 94 known and presumptive phenazine-producing strains representative of economically important groups of bacteria from diverse environmental and clinical habitats. Primers Ps_up1 and Ps_low1 (Table 2) amplified the predicted 427-bp *phzF* fragment from all 51 pseudomonads tested, including strains of *P. aeruginosa*, *P. chlororaphis* subsp. *chlororaphis*, *P. chlororaphis* subsp. *aureofaciens*, and *P. fluorescens* and 24 *Pseudomonas* strains of uncertain taxonomic affiliation. The latter group included 15 new phenazine-producing isolates from the rhizosphere of wheat collected near Ritzville and Lind, WA (Table 1). Of 27 *Burkholderia* strains, 15 were positive for *phzF* (Table 1) as determined by PCR with the *Burkholderia*-specific primers Bcep_up and Ps_low2 (Table 2). Unexpectedly, *Burkholderia phenazinium* ATCC 33666, described as a strain that produces the phenazine iodinin (64), was negative when a PCR was performed with these primers. Because this strain is described as a phenazine producer, we also screened genomic DNA from all 27 *Burkholderia* strains by performing high-stringency dot blot hybridization with three DNA probes spanning different parts of the *phz* operon from *B. lata* 383. In all cases, strains that were negative when PCR was used (including ATCC 33666) also were negative when hybridization was used (data not shown). The *phzF*-negative *Burkholderia* strains were also tested for production of PCA by thin-layer chromatography. Except for *B. phenazinium* ATCC 33666, the only strain that was positive for PCA, the results of the thin-layer chromatography- and PCR-based screens were in complete agreement (data not shown).

Eleven *Pectobacterium* strains representing three species were screened by performing PCR with two primer sets based on *phzF* sequences from *P. atrosepticum* and *P. agglomerans*. Only *P. atrosepticum* SCRI 1043 and *P. carotovorum* cc303 were positive when PCR was performed with the *Pectobacterium*-specific primers Ecar_up and Ecar_low, and amplification with the *Pantoea*-specific primers Paggl_up and Paggl_low identified only one positive strain, *Pectobacterium betavasculorum* Ecb168 (Table 1). All *phzF*-negative *Pectobacterium* strains also were negative for production of PCA when thin-layer chromatography was used (data not shown). Finally, genomic DNA samples from *Brevibacterium* and *Streptomyces* strains were screened with the oligonucleotide primer pairs Br_up/Br_low and Ps_up1/Ps_low2, respectively (Table 2). The Br_up/Br_low primer set yielded amplified *phzF* fragments for all strains of *B. iodinum* tested, and primers Ps_up1 and Ps_low2 amplified DNA from *S. cinnamonensis* DSM1042 (Table 1). The amplified DNA fragments obtained from the strains were sequenced and used in phylogenetic analyses, as outlined below.

Phylogeny of the core phenazine biosynthesis genes in *Pseudomonas* spp. A *phzF*-based phylogeny was derived by using a comprehensive data set that was strictly limited to functional homologues (i.e., homologues that were present in sequenced genomes and experimentally characterized loci and encoded enzymes that form part of a complete phenazine biosynthesis pathway). The data set contained 57 *phzF* nucleotide sequences generated in this study together with alleles previously deposited in the GenBank databases. The nonredundant and environmental GenBank databases included 15

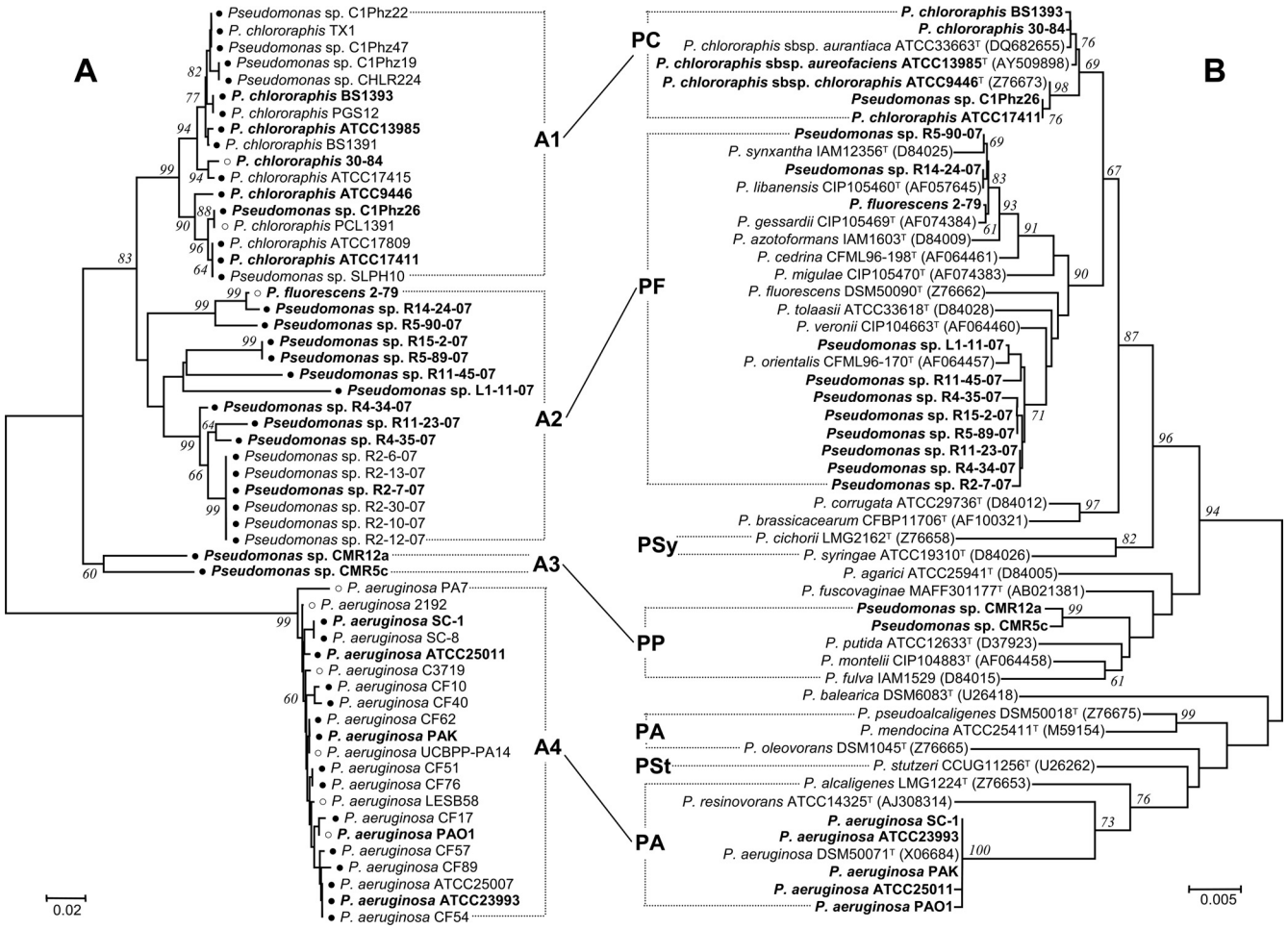

FIG. 1. Comparison of neighbor-joining phylogenies inferred from data for aligned 391-bp fragments of *phzF* (A) and 1,440-bp fragments of *rrs* (B) of *Pseudomonas* spp. In addition to sequences from phenazine-producing strains, the data set used to infer the 16S rRNA gene phylogeny included sequences from type strains of the *P. chlororaphis* (PC), *P. fluorescens* (PF), *P. syringae* (PSy), *P. putida* (PP), *P. aeruginosa* (PA), and *P. stutzeri* (PSt) species complexes as defined by Anzai et al. (4). Indels were ignored in the analysis, and evolutionary distances were estimated using the Kimura two-parameter model of nucleotide substitution. Bootstrap values greater than 60% are indicated at the nodes, and scale bars indicate substitutions per site. The branch lengths are proportional to the amount of evolutionary change. Sequences of *phzF* retrieved from the GenBank database and sequences generated in this study are indicated by open and filled circles, respectively. Phenazine-producing species used for further phylogenetic analyses are indicated by bold type.

phenazine biosynthesis operons, 10 of which originated from partially or completely sequenced bacterial genomes. The DNA sequence of the phenazine operon from *P. fluorescens* S2P5 (GenBank accession no. AY960782) was identical to that of *P. fluorescens* 2-79 (44), and it was not included. We also identified a 2.4-kb contig (GenBank accession no. AACY020165889) in the Sargasso Sea metagenome that contained a *phzF*-like open reading frame. The gene, however, appeared not to be a part of the phenazine biosynthesis pathway and was not included in further analyses. The resultant combined *phzF* data set ($n = 83$) was subjected to NJ and MP analyses, and based on this initial evaluation of diversity, we chose representative strains from each cluster (Table 1, bold type) for further phylogenetic analyses and topological comparisons.

Phylograms inferred from *Pseudomonas phzF* sequences revealed four clades designated clades A1 through A4 (Fig. 1A). Two of these clades, clades A1 and A4, were supported by high bootstrap values and contained *phzF* genes from strains of *P. chlororaphis* and *P. aeruginosa*, respectively. The A2 clade contained *phzF* genes from the model biocontrol strain *P. fluorescens* 2-79 together with *phzF* genes from phenazine-producing strains that we recently isolated from wheat grown in central Washington. Compared to clades A1 and A4, clade A2 was more diffuse, and it contained at least two subclades: one subclade formed by strains 2-79, R14-24-07, and R5-90-07 and a second subclade formed by strains R11-23-07, R4-X-07, and R2-X-07 (Fig. 1A). The fourth clade, clade A3, included only sequences obtained from strains CMR12a and CMR5c, which were isolated from cocoyam (49).

We also correlated the four groups defined by *phzF* with the established systematics of *Pseudomonas* species by comparing the 16S rRNA gene sequences of the phenazine producers to those of type strains representing species complexes as defined by Anzai et al. (4). The results indicated that strains that formed clades A1, A3, and A4 fell into the "*P. chlororaphis*,"

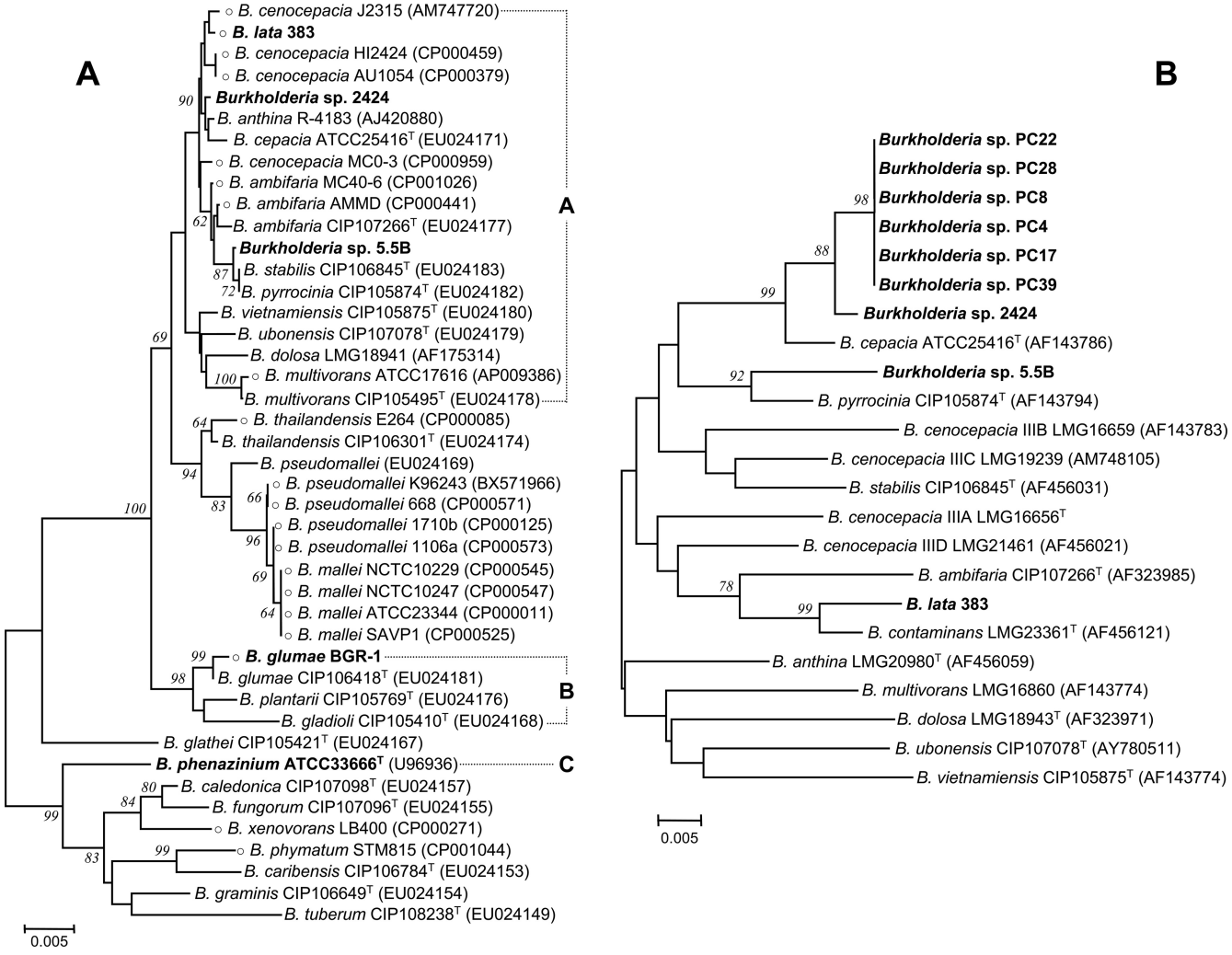

FIG. 2. Neighbor-joining phylogenies inferred from data for *rrs* sequences of *Burkholderia* spp. (A) and *recA* genes of the *B. cepacia* species complex (B). Indels were ignored, and the data sets used for analysis of *rrs* and *recA* contained 1,307 and 561 characters, respectively. Evolutionary distances were estimated using the Kimura two-parameter model of nucleotide substitution. Bootstrap values greater than 60% are indicated at the nodes, and the scale bar indicates 0.005 substitution per site. The branch lengths are proportional to the amount of evolutionary change. Phenazine-producing strains are indicated by bold type. Open circles indicate species whose genomes have been sequenced.

"*Pseudomonas putida*," and "*P. aeruginosa*" species complexes, respectively (Fig. 1B). The A2 clade corresponded to the "*P. fluorescens*" complex and again formed two subgroups, one corresponding to *Pseudomonas synxantha*, *Pseudomonas libanensis*, and *Pseudomonas gessardii* and the other corresponding to *Pseudomonas orientalis.*

Phylogeny of phenazine biosynthesis genes in *Burkholderia* spp. Phylograms inferred from *rrs* (Fig. 2A) and *phzF* (Fig. 3A) data revealed that phenazine genes are carried by strains in three distinct *rrs* clades and are highly conserved in *Burkholderia* spp. According to 16S rRNA gene analyses, the phenazine-producing strains sequenced in this study fell into clade A and clustered with species of the *Burkholderia cepacia* complex (Fig. 2). This complex includes at least 17 species that occupy diverse ecological niches and can cause human, animal, or plant diseases (65). These species are closely related and are commonly identified based on *recA* sequence and multilocus sequence typing analyses. *recA*-based dissection of clade A revealed that the newly sequenced strains 5.5B and 2424 (together with very similar strains PC4, PC8, PC17, PC22, PC28, and PC39) are closely related to *Burkholderia pyrrocinia* and *B. cepacia*, respectively (Fig. 2B), whereas strain 383, which was recently separated and placed in a new species called *B. lata* (65), is similar to *Burkholderia contaminans* and *Burkholderia ambifaria*. Clade B contained *Burkholderia plantarii*, *Burkholderia gladioli*, and *B. glumae* CIP106418, as well as the phenazine-producing strain *B. glumae* BGR-1 (Fig. 2A). Clade C was represented by a single phenazine-producing species, *B. phenazinium* ATCC 33666, for which we confirmed phenazine production but were unable to isolate and sequence core phenazine genes (Fig. 2A).

Analysis of genome regions flanking *phz* operons revealed that phenazine genes in *Burkholderia* spp. are associated with unique insertion sequence (IS) composite transposons. In *B. glumae* BGR-1, the phenazine genes are on chromosome 2 and are flanked by 32-bp imperfect inverted repeats and direct

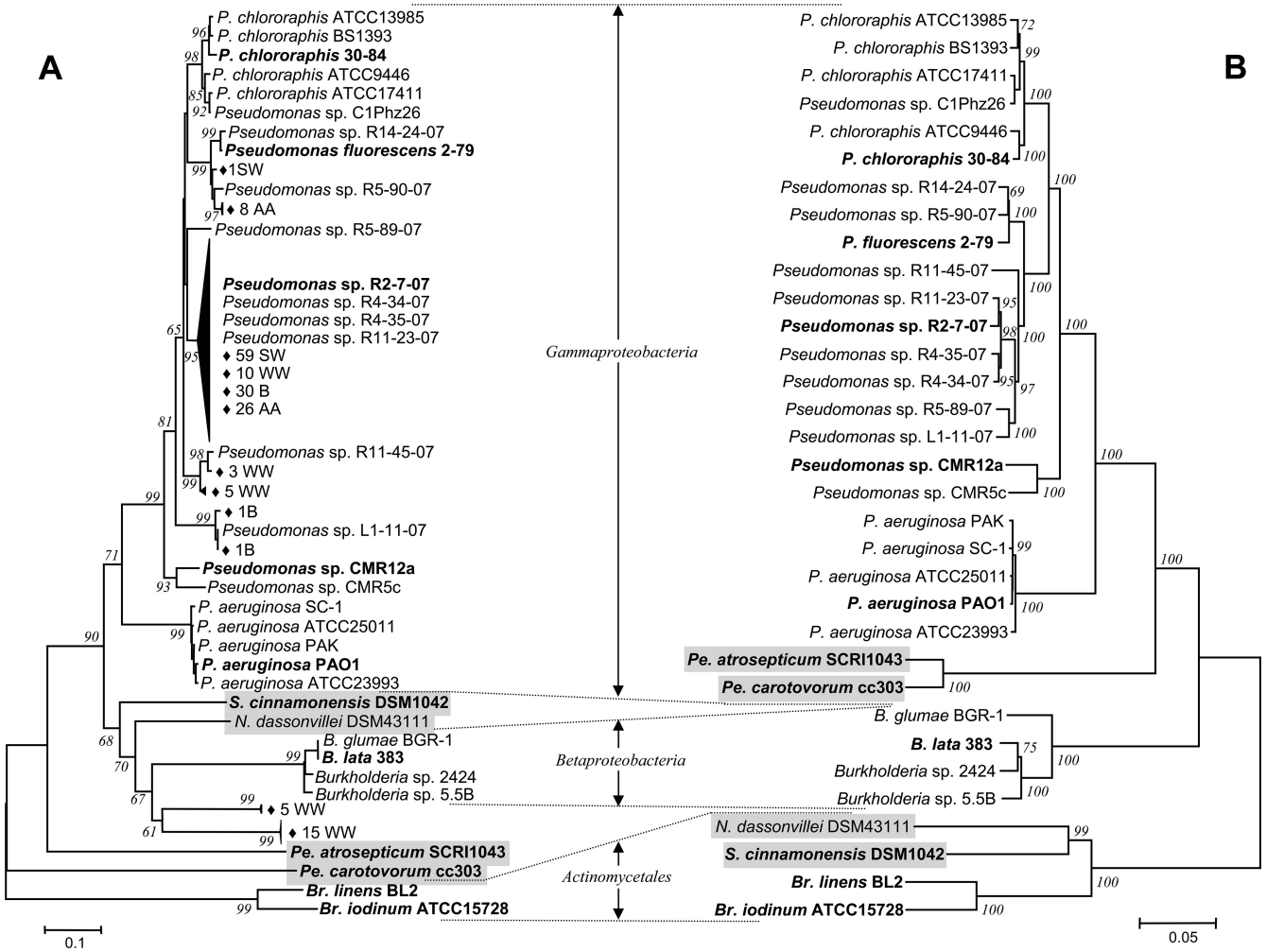

FIG. 3. Comparison of neighbor-joining phylogenies inferred from data for *phzF* (A) and concatenated housekeeping genes (*rrs*, *recA*, *rpoB*, *atpD*, and *gyrB*) (B) of the core set of phenazine-producing species. Indels were ignored in the analysis, and the *phzF* and concatenated housekeeping gene data sets contained 378 and 4,286 characters, respectively. Evolutionary distances were estimated using the Kimura two-parameter model of nucleotide substitution. The reproducibility of clades was assessed by bootstrap resampling with 1,000 pseudoreplicates, and bootstrap values greater than 60% are indicated at the nodes. The branch lengths are proportional to the amount of evolutionary change. The scale bars indicate substitution per site. Nodes with nearly identical sequences were collapsed. The *phzF* alleles originating from rhizosphere DNA are indicated by solid diamonds followed by a digit corresponding to the number of sequences in the collapsed node followed by a letter(s) indicating the crop (SW, spring wheat; WW, winter wheat; B, barley; AA, alfalfa) from which rhizosphere DNA was extracted. Shading indicates sequences that did not cluster similarly in the two trees. Bold type indicates organisms that were used for maximum likelihood and Bayesian analyses.

copies of the IS*402* transposase gene, one of which contains an internal frameshift (Fig. 4B). The putative transposon also carries a full-length IS*Rsp9* transposase gene and a truncated gene encoding a transposase of the IS*1421* family. The *phz* operon in *B. lata* 383 also is on chromosome 2 and is flanked by transposase genes of IS*1202* (Fig. 4B). The putative composite transposon is probably anchored in the genome since only the first transposase gene is intact and it is preceded by a 32-bp stretch of nucleotides that form the left end of IS*1202* (http://www-is.biotoul.fr), whereas the second transposase gene is truncated and lacks the right transposon end. The putative "phenazine transposon" in *B. lata* 383 forms part of a unique 49-kb DNA segment that is not present in the genomes of the closely related phenazine-nonproducing strains *B. ambifaria* AMMD (accession no. CP000441) and *B. ambifaria* MC40-6 (accession no. CP001026) (see Fig. S1 in the supplemental material). The *phz* operon occupies the center of the segment and is flanked by regions with low G+C contents and at least two putative operons with unknown functions.

We also screened regions flanking the *phz* operons in other groups of bacteria to look for evidence of recent horizontal gene transfer events. Comparison of the regions flanking phenazine operons of *P. aeruginosa* to sequences in phenazine-nonproducing *Pseudomonas* spp. revealed that there were no extended stretches with significant similarity. Similar results were obtained when sequences of *P. atrosepticum* SCRI1043 and the closely related phenazine-nonproducing strain *Erwinia tasmaniensis* Et1/99 were compared (32).

Phylogeny of the core *phz* genes in other groups of bacteria. To compare the phylogeny of *phzF* to that of the core bacterial

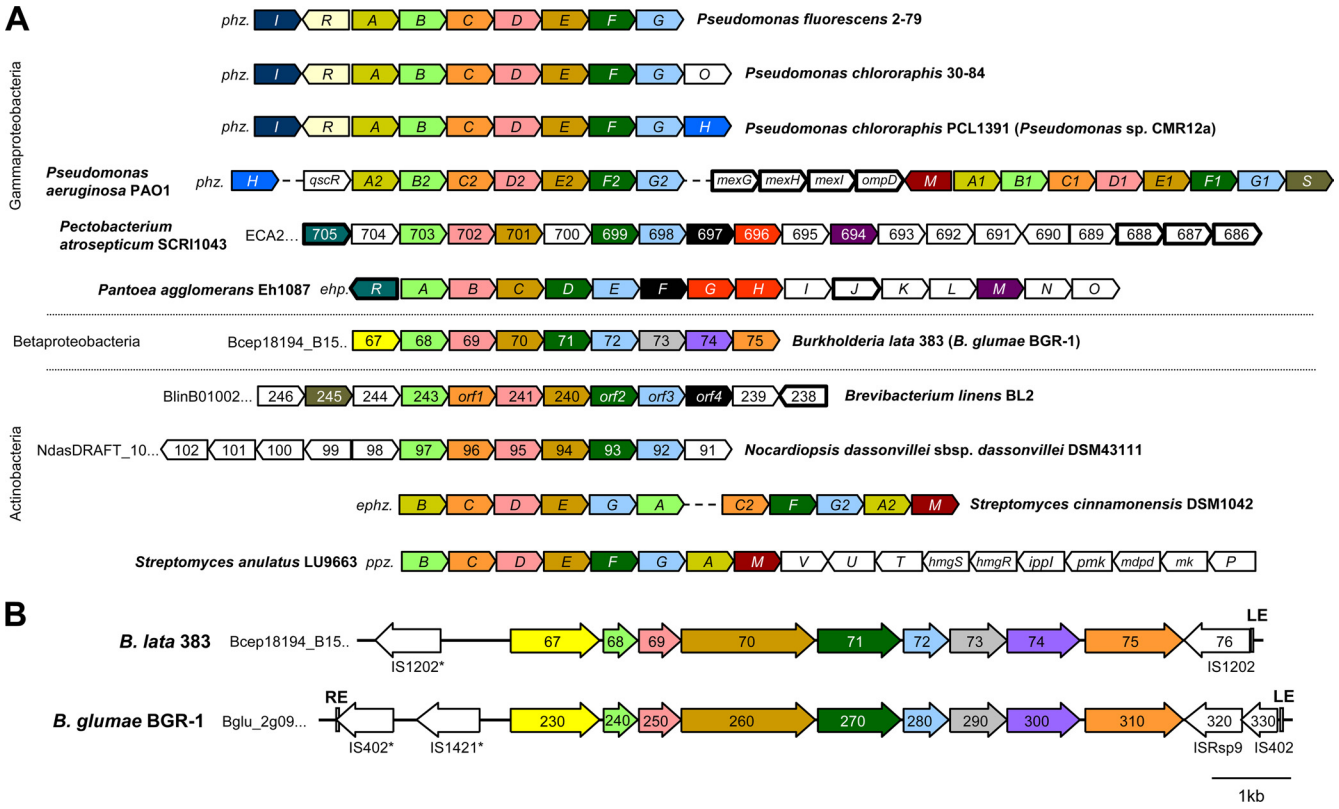

FIG. 4. Organization of the phenazine biosynthesis loci in different bacterial species (A) and physical maps of putative composite phenazine transposons from *Burkholderia* spp. (B). Genes and their orientations are indicated by arrows. Homologous genes in *P. fluorescens* 2-79 (44), *P. chlororaphis* 30-84 (44, 50), *P. chlororaphis* PCL1391 (14), *Pseudomonas* sp. CMR12a (M. Höfte, personal communication), *P. aeruginosa* PAO1 (59), *P. atrosepticum* SCRI1043 (7), *P. agglomerans* Eh1087 (21), *B. lata* 383, *B. glumae* BGR-1, *B. linens* BL2, *N. dassonvillei* subsp. *dassonvillei* DSM43111, *S. cinnamonensis* DMS1042 (24), and *S. anulatus* LU9663 (55) are indicated by arrows that are the same color, whereas unique species-specific genes are indicated by open arrows. For sequenced genomes, locus tags are indicated using a code; e.g., the locus tag for the *phzB* homologue of *B. lata* 383 is Bcep18194_B1568. In panel A, the sizes of genes and intergenic regions are not to scale, and the arrows with bold outlines indicate known or putative phenazine transport genes. In panel B, the open arrows represent intact and inactive (indicated by asterisks) transposase genes, and the rectangles indicate putative left (LE) and right (RE) transposon ends.

genome, we estimated phylogeny using five highly conserved housekeeping genes: *rrs*, *recA*, *rpoB*, *atpD*, and *gyrB*. These genes function in unrelated metabolic processes and encode the RNA component of the 30S ribosome subunit, the homologous recombination and DNA repair protein recombinase A, the β subunit of bacterial DNA-directed RNA polymerase, the catalytic β subunit of the F_0F_1-ATP synthase complex, and the B subunit of DNA gyrase (topoisomerase II), respectively.

The topology of the phylogram inferred using the concatenated housekeeping genes agreed with the accepted phylogeny of the taxa included in our analysis (Fig. 3B). Phylogenies estimated by different methods were highly congruent and revealed three major clades corresponding to members of the *Gammaproteobacteria* (*Pseudomonas* spp. and *Pectobacterium* spp.), *Betaproteobacteria* (*Burkholderia* spp.), and *Actinomycetales* (*S. cinnamonensis*, *N. dassonvillei*, and *Brevibacterium* spp.). In contrast, phylogenies inferred from *phzF* data were only partially congruent with the concatenated phylogeny (Fig. 3A). Most notably, *phzF* genes from *S. cinnamonensis* DSM1042 and *N. dassonvillei* DSM43111 clustered with the *Betaproteobacteria* genes, whereas the homologues from *P. carotovorum* cc303 and *P. atrosepticum* SCRI1043 formed separate nodes.

Data sets with a reduced number of taxa ($n = 13$) were constructed to facilitate more detailed ML phylogenetic analyses and topological comparisons of phylogenies estimated using different genomic regions. Isolates indicated by bold type in Fig. 3 were selected to represent each of the major clades revealed during preliminary distance analyses of all of the taxa sampled. The topologies of the combined housekeeping gene phylogenies estimated by the ML, Bayesian, parsimony, and distance methods were not significantly different ($0.277 < P < 1.000$). The topologies of the *phzF* trees estimated by the same four methods also were not significantly different ($0.207 < P < 0.266$). The topology of the combined ML phylogeny was compared to the topology of the *phzF* ML phylogeny by using SH tests with null distributions constructed in two ways. First, the *phzF* consensus topology was tested against the combined consensus topology with bootstrap resampling performed with the combined data set (885 characters). The second test involved comparison of the combined consensus topology with the *phzF* consensus topology with bootstrap resampling performed us-

ing the *phzF* data set (67 characters). Both tests demonstrated that the topology of the *phzF* phylogeny was significantly different ($P = 0.000$ and $P < 0.013$, respectively) from that of the combined phylogeny (see Fig. S2 in the supplemental material). The phylograms inferred from *phzF* data were also congruent with the phylograms inferred from the data for the *phzD*, *phzE*, and *phzG* core phenazine genes shared by all phenazine pathways and with the phylograms inferred from a concatenated data set for the four *phz* genes (data not shown).

Finally, we analyzed polymorphisms in *phzF* and the housekeeping genes in different groups of phenazine-producing bacteria. For all genera, the diversity of *phzF* sequences varied between 0.03 (*Burkholderia*) and 0.162 (*Pseudomonas*) and on average was slightly greater than the diversity of the corresponding housekeeping genes (see Table S1 in the supplemental material). The nucleotide diversity values for the housekeeping genes ranged from 0.003 (*rrs* from *Burkholderia*) to 0.173 (*gyrB* from *Brevibacterium*), and on average *rrs* and *gyrB* were the most and least conserved genes, respectively, for all taxa. The ratios of nonsynonymous substitutions to synonymous substitutions (dN/dS) exhibited a similar trend; the values obtained for *phzF* were higher (0.056 to 0.248) than those obtained for the housekeeping genes, for which the values were between 0.025 (*atpD* from *Brevibacterium*) and 0.085 (*gyrB* from *Brevibacterium*). All dN/dS ratios were <1, indicating that all genes, including *phzF*, were subjected to purifying selection (i.e., a form of natural selection that lowers the frequency of alleles with reduced fitness or viability in a population).

Organization and diversity of the phenazine pathways. A comparison of the sequences for *phz* operons clearly revealed that in all species the core biosynthesis genes are clustered and highly conserved (Fig. 4A). Minor variations in the organization of the core pathway include the absence of the 3-deoxy-D-arabino-heptulosonate-7-phosphate (DAHP) synthase-encoding gene *phzC* in the pathways of enteric bacteria and duplication of the *phzA*/*B* gene in pseudomonads and *S. cinnamonensis* DSM1042. Enzymes encoded by *phzB*, *phzD*, *phzE*, *phzF*, and *phzG* appear to be indispensable for synthesis of the phenazine scaffold and are present in all phenazine-producing species. Some bacteria, including *S. cinnamonensis* DSM1042 and strains of *P. aeruginosa*, contain two copies of the core pathway (23, 43). The core genes are often physically linked to various auxiliary genes encoding phenazine-modifying enzymes and efflux and regulatory proteins (42) (Fig. 4A). Compared to the parameters for the core genes, the distribution, orientation, proximity, and location of phenazine-modifying genes are highly variable, which means that they are of little value for phylogenetic inference. The putative phenazine efflux transporters include members of the ABC (*B. linens* BL2 and *P. atrosepticum* SCRI1043), proton motive force-dependent RND (*P. aeruginosa* PAO1), and major facilitator (*P. agglomerans* Eh1087) superfamilies. Finally, in most *Pseudomonas* spp., phenazine operons also are coupled with dedicated regulatory genes. In *P. chlororaphis*, *P. aeruginosa*, *Pseudomonas* sp. CMR12a, and strains of the *P. fluorescens* complex, the regulator genes *phzI* and *phzR* form a quorum-sensing circuit that regulates production of phenazines in relation to population density (42; M. Höfte, personal communication). The phylogeny of the *phzI* and *phzR* genes has recently been reported (37) and is not described here.

DISCUSSION

The work described in this paper required development of new probes targeting phenazine biosynthesis genes because the probes described previously (43) were based on sequences only from *Pseudomonas* and thus had a limited detection range. Using the new primers targeting *phzF*, a core biosynthesis gene common to all known phenazine-producing species, we screened 94 strains representing five genera and generated 57 new *phzF* sequences that, together with previous data, confirmed the remarkable diversity of phenazine-producing bacteria and at the same time revealed that most of them appear to be soil-dwelling and/or plant-associated species (Table 1). The latter conclusion is supported by our discovery of indigenous phenazine-producing bacteria in the rhizospheres of cereals collected near Lind and Ritzville, WA (Table 3). This is the first example of soils from the United States enriched in indigenous phenazine-producing bacteria and only the second such example in the world after the *Fusarium* wilt-suppressive soil of the Châteaurenard area in Dijon, France (45). Preliminary characterization suggested that phenazine-producing bacteria belonging to the *P. fluorescens* species complex (Fig. 1 and 3) are abundant in the Lind and Ritzville soils (10^5 to 10^6 CFU/g of root [data not shown]). The analysis of DNA extracted from the rhizosphere of winter wheat also revealed the presence of a novel group of phenazine producers whose *phzF* genes form two distinct clades clustering with *Actinobacteria* and *Burkholderia* spp. (Fig. 3A). Taken together, our findings suggest that phenazine producers may be ubiquitous and far more diverse in the environment than previously recognized.

Comparison of the various phenazine operons revealed high levels of similarity in the overall organization of the core biosynthesis genes and conservation of functions encoded by *phzD*, *phzE*, *phzF*, and *phzG* (Fig. 4A). A few notable differences include the lack of a PhzC homologue in pathways in *P. atrosepticum* (based on interrogation of the SCRI1043 genome) and *P. agglomerans* and the presence in core operons of *B. lata*, *B. glumae*, *B. linens*, *N. dassonvillei*, *P. atrosepticum*, and *P. agglomerans* of only one copy of the *phzA*/*B* homologue. PhzC is a putative DAHP synthase that is thought to act at the branch point of the shikimic acid pathway, probably to ensure abundant chorismate for phenazine synthesis (42) (see Fig. S3 in the supplemental material). The fact that *phzC* is not present in the operons of *P. atrosepticum* and *P. agglomerans* may reflect alternative routes leading to chorismate pools in these species or may indicate a level of phenazine synthesis lower than that in *Pseudomonas*. The presence or absence of a second copy of the *phzB* gene (designated *phzA*) is more intriguing and may be linked to production of different primary phenazine products.

All natural phenazines are derived from PCA and/or phenazine-1,6-dicarboxylic acid (PDC) (see Fig. S3 in the supplemental material), and evidence obtained previously suggests that phenazine-producing bacteria can be grouped into organisms that produce only PCA and organisms that produce PCA plus PDC (21, 48). A key step in formation of the phenazine scaffold involves the condensation of two molecules of amino-

cyclohexenone to form a tricyclic phenazine precursor via a reaction catalyzed by the small dimeric protein PhzB (2, 9) (see Fig. S3 in the supplemental material). Interestingly, all pseudomonads carry the *phzA* gene, which is very similar to *phzB* and encodes an enzymatically inactive paralogue. It has been suggested that this may lead to formation *in vivo* of a PhzA/B heterodimer with only one catalytically competent active center. Such an enzyme might allow rapid spontaneous oxidative decarboxylation of a transient tricyclic intermediate, resulting in formation of PCA instead of PDC. We hypothesize that the presence or absence of *phzA* is a global feature that separates pathways that form only PCA and pathways that form PCA plus PDC and ultimately predetermines the identity of phenazine compounds produced by various bacterial genera (Fig. 4A; see Fig. S3 in the supplemental material). Indeed, the comparison of core biosynthesis genes and naturally occurring phenazines revealed that both confirmed (*P. agglomerans* Eh1087) and proposed (*P. atrosepticum*, *Brevibacterium* spp., and *Burkholderia* spp.) PDC producers lack the *phzA* homologue and produce 1,6-disubstituted phenazines (21, 64), whereas *S. cinnamonensis* and all *Pseudomonas* spp. carry both *phzA* and *phzB* and produce phenazines that are derived from PCA (42, 64).

In *Streptomyces* and some closely related taxa, enzymes encoded by certain core phenazine genes are "recycled" in other biosynthesis pathways. Through interrogation of sequenced bacterial genomes we discovered homologues of *phzC*, *phzD*, and *phzE* in *Mycobacterium abscessus* (GenBank accession no. CU458896), *Streptomyces* sp. Mg1 (GenBank accession no. DS570398), and *Frankia* sp. EAN1pec (GenBank accession no. CP000820). Because these species lack orthologues of *phzB* and *phzF*, we suggest that these genes are not involved in phenazine biosynthesis but instead function in the synthesis of uncharacterized secondary metabolites or derivatives of shikimic and *trans*-2,3-dihydro-3-hydroxyanthranilic acids. One such pathway was recently described for the marine actinomycete *Micromonospora* sp. 046Eco-11, in which homologues of *phzC*, *phzD*, and *phzE* were implicated in the production of a novel antimicrobial alkaloid, diazepinomicin (47).

Our investigation of the phylogeny of the core phenazine biosynthesis genes focused first on fluorescent pseudomonads, the best-characterized group of phenazine producers. Two trends were immediately apparent when the evolutionary history of *phzF* was compared to that of the corresponding housekeeping genes. First, the topological congruence among the inferred evolutionary trees (Fig. 1 and 3) suggests that acquisition of the phenazine genes by pseudomonads was an early event, possibly preceding speciation in this group of bacteria. Second, our results underscore the emerging taxonomic diversity of phenazine-producing pseudomonads. It has long been recognized that phenazine synthesis occurs predominantly in strains of *P. chlororaphis*, *Pseudomonas aureofaciens* (now classified as *P. chlororaphis* subsp. *aureofaciens*), and *P. aeruginosa*. However, our analyses of housekeeping genes suggest that newly isolated phenazine-producing members of the *P. fluorescens* and *P. putida* species complexes (clusters PF and PP in Fig. 1) may belong to new species, raising questions about the actual number of *Pseudomonas* spp. capable of phenazine production. Further genetic and bioanalytical analyses are needed to clarify this issue.

Results of our analyses suggest that *phz* pathways may have evolved via horizontal gene transfer in some bacterial lineages. At least one event is ancient and best exemplified by the unequivocal clustering of the *phzF* genes from *Streptomyces* and *Nocardiopsis* (Gram-positive *Actinobacteria*) with their homologues from *Pseudomonas* spp. (Gram-negative *Gammaproteobacteria*) and *Burkholderia* spp. (Gram-negative *Betaproteobacteria*) (Fig. 3A; see Fig. S2 in the supplemental material). This pattern agrees with the findings of Fitzpatrick (19) but is not consistent with the generally accepted systematics of these genera (15) or with the phylogeny inferred from data for housekeeping genes in this study (Fig. 3B; see Fig. S2 in the supplemental material). In contrast to the situation in *Actinobacteria*, horizontal transfer of phenazine biosynthesis genes among species of *Burkholderia*, *Pectobacterium*, and *Pantoea* is probably still occurring and mediated by mobile genetic elements. Our results suggest that in *Burkholderia* spp. phenazine genes are dispersed by unique composite transposons similar to those found in the genomes of *B. lata* 383 and *B. glumae* BGR-1 (Fig. 4B). This hypothesis is supported by the unusually high degree of sequence conservation and the patchy distribution of *phz* genes among different *Burkholderia* spp. Interestingly, in members of the *B. cepacia* complex, the phenazine genes seem to be carried predominantly by species that include environmental isolates that are not highly prevalent in cystic fibrosis patients (i.e., *B. cepacia*, *B. pyrrocinia*, and *B. lata*) (38). We did not detect phenazine genes in strains of *Burkholderia cenocepacia*, *Burkholderia multivorans*, and *Burkholderia vietnamiensis*, which represent the most common groups of cystic fibrosis pathogens (Table 1). In contrast to the situation in *Burkholderia* spp., analysis of *phzF* from phenazine-producing *Pectobacterium* spp. revealed two very divergent gene variants exemplified by the genes found in *P. atrosepticum* SCRI1043 and *P. carotovorum* cc303. The estimated genetic distance between the *phzF* genes from these strains is far greater than one would expect in such close relatives (Fig. 3). In another closely related strain, *P. agglomerans* Eh1087, the phenazine biosynthesis genes are carried by a large indigenous plasmid (21), and in *P. atrosepticum* SCRI1043 the phenazine operon was identified as a genomic island (7).

We speculate that the conservation of phenazine genes in some bacteria, versus the active dissemination via horizontal transfer in other bacteria, reflects differences in the roles that phenazines play in microorganisms. Bacteria with highly conserved *phz* genes are exemplified by *Pseudomonas* spp., in which the functions of the genes likely include not only signaling but also antibiosis and extracellular electron shuttling, which can mediate mineral acquisition and the reoxidation of NADH under high-density oxygen-limited conditions, such as those that occur in mature biofilms (17, 18, 26, 39, 53). Consequently, large quantities of phenazines (milligrams to grams per liter *in vitro*) are produced by pseudomonads, and the biosynthesis pathways are enmeshed in the metabolism and tightly regulated (42). At the opposite end of the spectrum are phenazine-producing species like *P. agglomerans* Eh1087, in which the *phz* genes are in a plasmid. The pathway in Eh1087 does not include a dedicated DAHP synthase, which probably results in lower phenazine yields. The main phenazine product, D-alanylgriseoluteic acid (AGA), acts in *P. agglomerans* like a typical antibiotic and is employed in competition with closely

related bacterial species in its ecological niche (22). Interestingly, AGA itself is toxic to *P. agglomerans* Eh1087, and the *phz* pathway encodes a special phenazine-binding protein, EhpR, that prevents self-poisoning of the producer (21). The diversity and patchy distribution of phenazine-modifying genes may also reflect the connection between the types of phenazine compounds produced by individual species and their habitats.

ACKNOWLEDGMENTS

We are grateful to Joyce E. Loper (USDA-ARS, Corvallis, OR), Monica Höfte (Ghent University, Ghent, Belgium), Gee W. Lau (University of Illinois at Urbana-Champaign, Urbana, IL), Kenichi Tsuchiya (Kyushu University, Fukuoka, Japan), and Shaji Philip (Rubber Research Institute of India, Kottayam, India) for providing bacterial strains used in this study and to Karen J. Adams for excellent technical assistance.

REFERENCES

1. **Abken, H. J., M. Tietze, J. Brodersen, S. Baumer, U. Beifuss, and U. Deppenmeier.** 1998. Isolation and characterization of methanophenazine and function of phenazines in membrane-bound electron transport of *Methanosarcina mazei* Gol. J. Bacteriol. **180:**2027–2032.
2. **Ahuja, E. G., P. Janning, M. Mentel, A. Graebsch, R. Breinbauer, W. Hiller, B. Costisella, L. S. Thomashow, D. V. Mavrodi, and W. Blankenfeldt.** 2008. PhzA/B catalyzes the formation of the tricycle in phenazine biosynthesis. J. Am. Chem. Soc. **130:**17053–17061.
3. **Akaike, H.** 1974. A new look at the statistical model identification. IEEE Trans. Automat. Control **19:**716–723.
4. **Anzai, Y., H. Kim, J. Y. Park, H. Wakabayashi, and H. Oyaizu.** 2000. Phylogenetic affiliation of the pseudomonads based on 16S rRNA sequence. Int. J. Syst. Evol. Microbiol. **50:**1563–1589.
5. **Ausubel, F. M., R. Brent, R. E. Kingston, D. D. Moore, J. G. Seidman, J. A. Smith, and S. K.** 2002. Short protocols in molecular biology, 5th ed. John Wiley and Sons, New York, NY.
6. **Axelrood, P. E., M. Rella, and M. N. Schroth.** 1988. Role of antibiosis in competition of *Erwinia* strains in potato infection courts. Appl. Environ. Microbiol. **54:**1222–1229.
7. **Bell, K. S., M. Sebaihia, L. Pritchard, M. T. Holden, L. J. Hyman, M. C. Holeva, N. R. Thomson, S. D. Bentley, L. J. Churcher, K. Mungall, R. Atkin, N. Bason, K. Brooks, T. Chillingworth, K. Clark, J. Doggett, A. Fraser, Z. Hance, H. Hauser, K. Jagels, S. Moule, H. Norbertczak, D. Ormond, C. Price, M. A. Quail, M. Sanders, D. Walker, S. Whitehead, G. P. Salmond, P. R. Birch, J. Parkhill, and I. K. Toth.** 2004. Genome sequence of the enterobacterial phytopathogen *Erwinia carotovora* subsp. *atroseptica* and characterization of virulence factors. Proc. Natl. Acad. Sci. U. S. A. **101:** 11105–11110.
8. **Bennett-Lovsey, R. M., A. D. Herbert, M. J. Sternberg, and L. A. Kelley.** 2008. Exploring the extremes of sequence/structure space with ensemble fold recognition in the program Phyre. Proteins **70:**611–625.
9. **Blankenfeldt, W., A. P. Kuzin, T. Skarina, Y. Korniyenko, L. Tong, P. Bayer, P. Janning, L. S. Thomashow, and D. V. Mavrodi.** 2004. Structure and function of the phenazine biosynthetic protein PhzF from *Pseudomonas fluorescens*. Proc. Natl. Acad. Sci. U. S. A. **101:**16431–16436.
10. **Bull, C. T., C. A. Ishimaru, and J. E. Loper.** 1994. Two genomic regions involved in catechol siderophore production by *Erwinia carotovora*. Appl. Environ. Microbiol. **60:**662–669.
11. **Cartwright, D. K., W. S. Chilton, and D. M. Benson.** 1995. Pyrrolnitrin and phenazine production by *Pseudomonas cepacia* strain 5.5B, a biocontrol agent of *Rhizoctonia solani*. Appl. Microbiol. Biotechnol. **43:**211–216.
12. **Carver, T. J., K. M. Rutherford, M. Berriman, M. A. Rajandream, B. G. Barrell, and J. Parkhill.** 2005. ACT: the Artemis Comparison Tool. Bioinformatics **21:**3422–3423.
13. **Chin-A-Woeng, T. F. C., G. V. Bloemberg, I. H. M. Mulders, L. C. Dekkers, and B. J. J. Lugtenberg.** 2000. Root colonization by phenazine-1-carboxamide-producing bacterium *Pseudomonas chlororaphis* PCL1391 is essential for biocontrol of tomato foot and root rot. Mol. Plant Microbe Interact. **13:** 1340–1345.
14. **Chin-A-Woeng, T. F. C., J. E. Thomas-Oates, B. J. J. Lugtenberg, and G. V. Bloemberg.** 2001. Introduction of the *phzH* gene of *Pseudomonas chlororaphis* PCL1391 extends the range of biocontrol ability of phenazine-1-carboxylic acid-producing *Pseudomonas* spp. strains. Mol. Plant Microbe Interact. **14:**1006–1015.
15. **Ciccarelli, F. D., T. Doerks, C. von Mering, C. J. Creevey, B. Snel, and P. Bork.** 2006. Toward automatic reconstruction of a highly resolved tree of life. Science **311:**1283–1287.
16. **Coenye, T., P. Vandamme, J. J. LiPuma, J. R. Govan, and E. Mahenthiralingam.** 2003. Updated version of the *Burkholderia cepacia* complex experimental strain panel. J. Clin. Microbiol. **41:**2797–2798.
17. **Dietrich, L. E., T. K. Teal, A. Price-Whelan, and D. K. Newman.** 2008. Redox-active antibiotics control gene expression and community behavior in divergent bacteria. Science **321:**1203–1206.
18. **Dietrich, L. E. P., A. Price-Whelan, A. Petersen, M. Whiteley, and D. K. Newman.** 2006. The phenazine pyocyanin is a terminal signalling factor in the quorum sensing network of *Pseudomonas aeruginosa*. Mol. Microbiol. **61:** 1308–1321.
19. **Fitzpatrick, D. A.** 2009. Lines of evidence for horizontal gene transfer of a phenazine producing operon into multiple bacterial species. J. Mol. Evol. **68:**171–185.
20. **Georgakopoulos, D. G., M. Hendson, N. J. Panopoulos, and M. N. Schroth.** 1994. Cloning of a phenazine biosynthetic locus of *Pseudomonas aureofaciens* PGS12 and analysis of its expression in vitro with the ice nucleation reporter gene. Appl. Environ. Microbiol. **60:**2931–2938.
21. **Giddens, S. R., Y. J. Feng, and H. K. Mahanty.** 2002. Characterization of a novel phenazine antibiotic gene cluster in *Erwinia herbicola* Eh1087. Mol. Microbiol. **45:**769–783.
22. **Giddens, S. R., G. J. Houliston, and H. K. Mahanty.** 2003. The influence of antibiotic production and pre-emptive colonization on the population dynamics of *Pantoea agglomerans* (*Erwinia herbicola*) Eh1087 and *Erwinia amylovora* in planta. Environ. Microbiol. **5:**1016–1021.
23. **Haagen, Y.** 2007. Molecular and biochemical analyses of biosynthesis of phenazine and furanonaphthoquinone I in *Streptomyces cinnamonensis* DSM 1042. Ph.D. thesis. Eberhard Karls University, Tubingen, Germany.
24. **Haagen, Y., K. Gluck, K. Fay, B. Kammerer, B. Gust, and L. Heide.** 2006. A gene cluster for prenylated naphthoquinone and prenylated phenazine biosynthesis in *Streptomyces cinnamonensis* DSM 1042. Chembiochem **7:**2016–2027.
25. **Hall, B. G.** 2004. Phylogenetic trees made easy: a how-to manual. Sinauer Associates, Sunderland, MA.
26. **Hernandez, M. E., A. Kappler, and D. K. Newman.** 2004. Phenazines and other redox-active antibiotics promote microbial mineral reduction. Appl. Environ. Microbiol. **70:**921–928.
27. **Huelsenbeck, J. P., J. J. Bull, and C. W. Cunningham.** 1996. Combining data in phylogenetic analysis. Trends Ecol. Evol. **11:**152–158.
28. **Huelsenbeck, J. P., and F. Ronquist.** 2001. MRBAYES: Baysian inference of phylogenetic trees. Bioinformatics **17:**754–755.
29. **Jones, D. T., W. R. Taylor, and J. M. Thornton.** 1992. The rapid generation of mutation data matrices from protein sequences. Comput. Appl. Biosci. **8:**275–282.
30. **Kimura, M.** 1980. A simple method for estimating evolutionary rates of base substitutions through comparative studies of nucleotide sequences. J. Mol. Evol. **16:**111–120.
31. **King, E. O., M. K. Ward, and D. E. Raney.** 1954. Two simple media for the demonstration of pyocyanin and fluorescein. J. Lab. Clin. Med. **44:**301–307.
32. **Kube, M., A. M. Migdoll, I. Muller, H. Kuhl, A. Beck, R. Reinhardt, and K. Geider.** 2008. The genome of *Erwinia tasmaniensis* strain Et1/99, a nonpathogenic bacterium in the genus *Erwinia*. Environ. Microbiol. **10:**2211–2222.
33. **Larkin, M. A., G. Blackshields, N. P. Brown, R. Chenna, P. A. McGettigan, H. McWilliam, F. Valentin, I. M. Wallace, A. Wilm, R. Lopez, J. D. Thompson, T. J. Gibson, and D. G. Higgins.** 2007. Clustal W and Clustal X version 2.0. Bioinformatics **23:**2947–2948.
34. **Larsen, G. Y., T. L. Stull, and J. L. Burns.** 1993. Marked phenotypic variability in *Pseudomonas cepacia* isolated from a patient with cystic fibrosis. J. Clin. Microbiol. **31:**788–792.
35. **Lau, G. W., H. M. Ran, F. S. Kong, D. J. Hassett, and D. Mavrodi.** 2004. *Pseudomonas aeruginosa* pyocyanin is critical for lung infection in mice. Infect. Immun. **72:**4275–4278.
36. **Laursen, J. B., and J. Nielsen.** 2004. Phenazine natural products: biosynthesis, synthetic analogues, and biological activity. Chem. Rev. **104:**1663–1685.
37. **Lerat, E., and N. A. Moran.** 2004. The evolutionary history of quorum-sensing systems in bacteria. Mol. Biol. Evol. **21:**903–913.
38. **LiPuma, J. J.** 2005. Update on the *Burkholderia cepacia* complex. Curr. Opin. Pulm. Med. **11:**528–533.
39. **Maddula, V. S., E. A. Pierson, and L. S. Pierson III.** 2008. Altering the ratio of phenazines in *Pseudomonas chlororaphis* (*aureofaciens*) strain 30-84: effects on biofilm formation and pathogen inhibition. J. Bacteriol. **190:**2759–2766.
40. **Mahajan-Miklos, S., M. W. Tan, L. G. Rahme, and F. M. Ausubel.** 1999. Molecular mechanisms of bacterial virulence elucidated using a *Pseudomonas aeruginosa-Caenorhabditis elegans* pathogenesis model. Cell **96:**47–56.
41. **Mahenthiralingam, E., T. Coenye, J. W. Chung, D. P. Speert, J. R. Govan, P. Taylor, and P. Vandamme.** 2000. Diagnostically and experimentally useful panel of strains from the *Burkholderia cepacia* complex. J. Clin. Microbiol. **38:**910–913.
42. **Mavrodi, D. V., W. Blankenfeldt, and L. S. Thomashow.** 2006. Phenazine compounds in fluorescent *Pseudomonas* spp.: biosynthesis and regulation. Annu. Rev. Phytopathol. **44:**417–445.
43. **Mavrodi, D. V., R. F. Bonsall, S. M. Delaney, M. J. Soule, G. Phillips, and L. S. Thomashow.** 2001. Functional analysis of genes for biosynthesis of

pyocyanin and phenazine-1-carboxamide from *Pseudomonas aeruginosa* PAO1. J. Bacteriol. **183:**6454–6465.

44. **Mavrodi, D. V., V. N. Ksenzenko, R. F. Bonsall, R. J. Cook, A. M. Boronin, and L. S. Thomashow.** 1998. A seven-gene locus for synthesis of phenazine-1-carboxylic acid by *Pseudomonas fluorescens* 2-79. J. Bacteriol. **180:**2541–2548.
45. **Mazurier, S., T. Corberand, P. Lemanceau, and J. M. Raaijmakers.** 2009. Phenazine antibiotics produced by fluorescent pseudomonads contribute to natural soil suppressiveness to Fusarium wilt. ISME J. **3:**977–991.
46. **Mazzola, M., R. J. Cook, L. S. Thomashow, D. M. Weller, and L. S. Pierson.** 1992. Contribution of phenazine antibiotic biosynthesis to the ecological competence of fluorescent pseudomonads in soil habitats. Appl. Environ. Microbiol. **58:**2616–2624.
47. **McAlpine, J. B., A. H. Banskota, R. D. Charan, G. Schlingmann, E. Zazopoulos, M. Piraee, J. Janso, V. S. Bernan, M. Aouidate, C. M. Farnet, X. Feng, Z. Zhao, and G. T. Carter.** 2008. Biosynthesis of diazepinomicin/ECO-4601, a *Micromonospora* secondary metabolite with a novel ring system. J. Nat. Prod. **71:**1585–1590.
48. **McDonald, M., D. V. Mavrodi, L. S. Thomashow, and H. G. Floss.** 2001. Phenazine biosynthesis in *Pseudomonas fluorescens*: branchpoint from the primary shikimate biosynthetic pathway and role of phenazine-1,6-dicarboxylic acid. J. Am. Chem. Soc. **123:**9459–9460.
49. **Perneel, M., J. Heyrman, A. Adiobo, K. De Maeyer, J. M. Raaijmakers, P. De Vos, and M. Hofte.** 2007. Characterization of CMR5c and CMR12a, novel fluorescent *Pseudomonas* strains from the cocoyam rhizosphere with biocontrol activity. J. Appl. Microbiol. **103:**1007–1020.
50. **Pierson, L. S., T. Gaffney, S. Lam, and F. C. Gong.** 1995. Molecular analysis of genes encoding phenazine biosynthesis in the biological control bacterium *Pseudomonas aureofaciens* 30-84. FEMS Microbiol. Lett. **134:**299–307.
51. **Posada, D.** 2006. ModelTest Server: a web-based tool for the statistical selection of models of nucleotide substitution online. Nucleic Acids Res. **34:**W700–W703.
52. **Price, E. W., and I. Carbone.** 2005. SNAP: workbench management tool for evolutionary population genetic analysis. Bioinformatics **21:**402–404.
53. **Price-Whelan, A., L. E. Dietrich, and D. K. Newman.** 2006. Rethinking 'secondary' metabolism: physiological roles for phenazine antibiotics. Nat. Chem. Biol. **2:**71–78.
54. **Rahme, L. G., F. M. Ausubel, H. Cao, E. Drenkard, B. C. Goumnerov, G. W. Lau, S. Mahajan-Miklos, J. Plotnikova, M. W. Tan, J. Tsongalis, C. L. Walendziewicz, and R. G. Tompkins.** 2000. Plants and animals share functionally common bacterial virulence factors. Proc. Natl. Acad. Sci. U. S. A. **97:**8815–8821.
55. **Saleh, O., B. Gust, B. Boll, H. P. Fiedler, and L. Heide.** 2009. Aromatic prenylation in phenazine biosynthesis: dihydrophenazine-1-carboxylate dimethylallyltransferase from *Streptomyces anulatus*. J. Biol. Chem. **284:**14439–14447.
56. **Seo, S. T., and K. Tsuchiya.** 2004. PCR-based identification and characterization of *Burkholderia cepacia* complex bacteria from clinical and environmental sources. Lett. Appl. Microbiol. **39:**413–419.
57. **Shimodaira, H., and M. Hasegawa.** 1999. Multiple comparisons of log-likelihoods with applications to phylogenetic inference. Mol. Biol. Evol. **16:**1114–1116.
58. **Stanier, R. Y., N. J. Palleroni, and M. Doudoroff.** 1966. The aerobic pseudomonads: a taxonomic study. J. Gen. Microbiol. **43:**159–271.
59. **Stover, C. K., X. Q. Pham, A. L. Erwin, S. D. Mizoguchi, P. Warrener, M. J. Hickey, F. S. Brinkman, W. O. Hufnagle, D. J. Kowalik, M. Lagrou, R. L. Garber, L. Goltry, E. Tolentino, S. Westbrock-Wadman, Y. Yuan, L. L. Brody, S. N. Coulter, K. R. Folger, A. Kas, K. Larbig, R. Lim, K. Smith, D. Spencer, G. K. Wong, Z. Wu, I. T. Paulsen, J. Reizer, M. H. Saier, R. E. Hancock, S. Lory, and M. V. Olson.** 2000. Complete genome sequence of *Pseudomonas aeruginosa* PAO1, an opportunistic pathogen. Nature **406:**959–964.
60. **Swofford, D. L.** 2002. PAUP*: phylogenetic analysis using parsimony (* and other methods), 4.0b10 ed. Sinauer Associates, Sunderland, MA.
61. **Tamura, K., J. Dudley, M. Nei, and S. Kumar.** 2007. MEGA4: Molecular Evolutionary Genetics Analysis (MEGA) software version 4.0. Mol. Biol. Evol. **24:**1596–1599.
62. **Thomashow, L. S., and D. M. Weller.** 1988. Role of a phenazine antibiotic from *Pseudomonas fluorescens* in biological control of *Gaeumannomyces graminis* var. *tritici*. J. Bacteriol. **170:**3499–3508.
63. **Thomashow, L. S., D. M. Weller, R. F. Bonsall, and L. S. Pierson.** 1990. Production of the antibiotic phenazine-1-carboxylic acid by fluorescent *Pseudomonas* species in the rhizosphere of wheat. Appl. Environ. Microbiol. **56:**908–912.
64. **Turner, J. M., and A. J. Messenger.** 1986. Occurrence, biochemistry and physiology of phenazine pigment production. Adv. Microb. Physiol. **27:**211–275.
65. **Vanlaere, E., A. Baldwin, D. Gevers, D. Henry, E. De Brandt, J. J. LiPuma, E. Mahenthiralingam, D. P. Speert, C. Dowson, and P. Vandamme.** 2009. Taxon K, a complex within the *Burkholderia cepacia* complex, comprises at least two novel species, *Burkholderia contaminans* sp. nov. and *Burkholderia lata* sp. nov. Int. J. Syst. Evol. Microbiol. **59:**102–111.
66. **Weisburg, W. G., S. M. Barns, D. A. Pelletier, and D. J. Lane.** 1991. 16S ribosomal DNA amplification for phylogenetic study. J. Bacteriol. **173:**697–703.
67. **Weller, D. M.** 1983. Colonization of wheat roots by a fluorescent pseudomonad suppressive to take-all. Phytopathology **73:**1548–1553.